Kelvin-Helmholtz instability for a bounded plasma flow in a longitudinal magnetic field

T. Burinskaya, M. Shevelev, Jean-Louis Rauch

Original Russian Text © T.M. Burinskaya, M.M. Shevelev, J.-L. Rauch, 2011, published in Fizika Plazmy, 2011, Vol. 37, No. 1, pp. 46–59.

Kelvin–Helmholtz Instability for a Bounded Plasma Flow in a Longitudinal Magnetic Field

T. M. Burinskaya[a], M. M. Shevelev[a], and J.-L. Rauch[b]

[a] *Space Research Institute, Russian Academy of Sciences, Profsoyuznaya ul. 84/32, Moscow, 117997 Russia*

[b] *Laboratoire de Physique et Chimie de l'Environnement et de l'Espace, Centre National de la Recherche Scientifique, av. de la Recherche Scientifique 3a, 45071 Orléans cedex 2, France*

Received April 26, 2010

Abstract—Kelvin–Helmholtz MHD instability in a plane three-layer plasma is investigated. A general dispersion relation for the case of arbitrarily orientated magnetic fields and flow velocities in the layers is derived, and its solutions for a bounded plasma flow in a longitudinal magnetic field are studied numerically. Analysis of Kelvin–Helmholtz instability for different ion acoustic velocities shows that perturbations with wavelengths on the order of or longer than the flow thickness can grow in an arbitrary direction even at a zero temperature. Oscillations excited at small angles with respect to the magnetic field exist in a limited range of wavenumbers even without allowance for the finite width of the transition region between the flow and the ambient plasma. It is shown that, in a low-temperature plasma, solutions resulting in kink-like deformations of the plasma flow grow at a higher rate than those resulting in quasi-symmetric (sausage-like) deformations. The transverse structure of oscillatory–damped eigenmodes in a low-temperature plasma is analyzed. The results obtained are used to explain mechanisms for the excitation of ultra-low-frequency long-wavelength oscillations propagating along the magnetic field in the plasma sheet boundary layer of the Earth's magnetotail penetrated by fast plasma flows.

DOI: 10.1134/S1063780X10111029

1. INTRODUCTION

Experimental data obtained using spacecrafts have shown that there are domains in the Earth's magnetosphere in which plasma flows are accompanied by low-frequency electromagnetic oscillations. Examples of such domains are the inner boundary of the transition region between the magnetosphere and the separated shock wave [1, 2], the central plasma sheet, the flank boundaries of the magnetotail, and the boundary region of the magnetotail plasma sheet [3–5]. Analysis of the experimental data presented in those papers indicates that Kelvin–Helmholtz instability (KHI) can play a decisive role in the generation of the observed electromagnetic oscillations.

KHI is one of the strongest hydrodynamic instabilities, and there are a large number of studies devoted to its analysis (see [6]). However, in most papers, stability of a plane interface between two unbounded plasmas propagating with respect to one another has been considered. Actually, plasma flows are always bounded in the transverse (with respect to the flow) direction and the ambient plasma can be inhomogeneous. Obviously, in order to investigate generation of oscillations with wavelengths substantially exceeding the transverse size of the flow, it is necessary to consider KHI in a system with several boundaries. The simplest model of such a system is a plane three-layer plasma in which one of the layers has a finite transverse size (see Fig. 1). KHI in a plane three-layer geometry was analyzed in [7] for an incompressible plasma with the same parameters on both sides of the flow. In [8], KHI in a three-layer compressible plasma system with longitudinal magnetic fields was studied numerically for some particular cases; however, for the parameter values used in that paper, the flow velocity was lower than the doubled ion-acoustic velocity. The choice of such parameters agrees with the results of the analysis of a

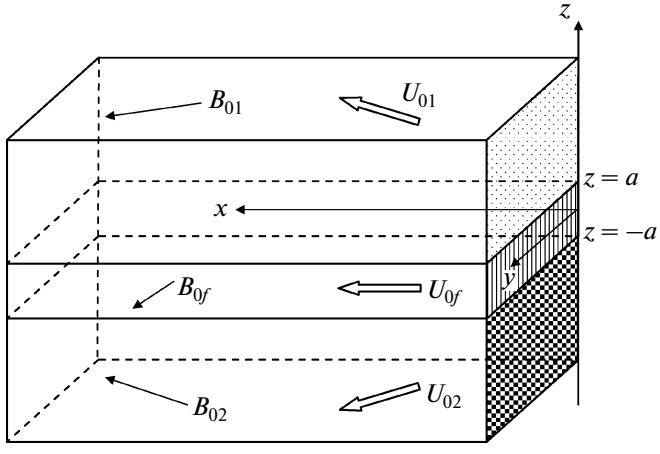

Fig. 1. Geometry of the model.

conventional problem in which two plasmas propagating with respect to one another along a magnetic field or at a relatively small angle to it are unstable only for the acoustic Mach number lower than 2. In this case, the flow velocity should be at least two times higher than the Alfvén velocity [9]. Thus, in a two-plasma system in a longitudinal magnetic field, the generation of waves with wave vectors directed along the magnetic field is possible only if the ion acoustic velocity is higher than the Alfvén velocity. This condition is, however, not satisfied in the plasma sheet boundary layer of the Earth's magnetotail, separating the cold rarefied lobe plasma from the hotter and denser plasma of the plasma sheet. However, analysis of the experimental data shows that it is in this region that long-wavelength oscillations of the magnetic field [5, 10] are detected simultaneously with fast (2000–3000 km/s) plasma flows propagating along the magnetic field.

The observed oscillations propagate mainly along the magnetic field with a velocity on the order of the local Alfvén velocity. The oscillation frequencies are in the range of 0.004–0.02 Hz; i.e., they are much lower than the ion cyclotron frequency. Typical oscillation wavelengths are in the range of 5–20 Earth's radii, and the typical size of the plasma sheet boundary layer in which fast plasma flows are observed is on the order of the Earth's radius in the North–South direction (the z axis in Fig. 1). The flow length in the dawn–dusk direction (the y axis in Fig. 1) is not determined precisely. According to estimates, it can be on the order of the flow size along the z axis or longer. Assuming that the flow length along the y axis is much larger than that along the z axis, the possibility of excitation of oscillations with wave vectors directed along the magnetic field for an arbitrary ratio between the Alfvén and ion acoustic velocities in a plane three-layer plasma system due to the onset of KHI was considered in [11]. It was shown that, in such a system, longitudinal oscillations can develop even if the ion acoustic velocity is much lower than the Alfvén velocity. Thus, in order to adequately describe the generation of long-wavelength oscillations in a low-temperature plasma, it is necessary to take into account the finite size of the propagating plasma flow.

In this paper, we continue our previous study of KHI in plane three-layer geometry [11]. Here, we consider stability of the plasma flow against the excitation of long-wavelength oscillations with arbitrarily directed wave vectors under the conditions typical of the plasma sheet boundary layer of the Earth's magnetotail, in which magnetic fields in all domains are directed along the plasma flow propagating in the bounded layer. The structure of the oscillation eigenmodes and the deformation of the flow boundaries due to the onset of KHI are analyzed.

Taking into account that the model developed here can be used to describe generation of low-frequency oscillations in other domains of the Earth's magnetosphere, e.g., in the magnetotail flanks, where plasma flows propagate in crossed magnetic fields, a general dispersion relation is derived for the case of arbitrarily oriented magnetic fields and flow velocities.

2. FORMULATION OF THE PROBLEM AND BASIC EQUATIONS

We consider stability of a plasma flow in a three-layer system schematically shown in Fig. 1. The system is divided into three domains along the z axis: $z > a$, $a > z > -a$, and $z < -a$. Within each domain, plasma is homogeneous, but the plasma parameters may be different in different domains. We denote the unperturbed flow velocities and magnetic fields in the domains by $\mathbf{U}_{0j}$ and $\mathbf{B}_{0j}$ ($j = 1, f, 2$), where the indices $1, f$, and 2 refer to the domains $z > a$, $a > z > -a$, and $z < -a$, respectively. The equilibrium flow velocities and magnetic fields in all three domains are parallel to the (x, y) plane. It is assumed that the plasma flow velocity in the bounded layer ($a > z > -a$) is directed along the x axis. Denoting the angles between the x axis and the vectors $\mathbf{B}_{0j}$ and $\mathbf{U}_{0j}$ by ζ_j and φ_j, respectively (with $\varphi_f \equiv 0$), we represent the vectors $\mathbf{B}_{0j}$ and $\mathbf{U}_{0j}$ as

$$\begin{aligned}
\mathbf{B}_{01} &= (B_{01}\cos\zeta_1, B_{01}\sin\zeta_1, 0),\\
\mathbf{B}_{02} &= (B_{02}\cos\zeta_2, B_{02}\sin\zeta_2, 0),\\
\mathbf{B}_{0f} &= (B_{0f}\cos\zeta_f, B_{0f}\sin\zeta_f, 0),\\
\mathbf{U}_{01} &= (U_{01}\cos\varphi_1, U_{01}\sin\varphi_1, 0),\\
\mathbf{U}_{02} &= (U_{02}\cos\varphi_2, U_{02}\sin\varphi_2, 0),\\
\mathbf{U}_{0f} &= (U_{0f}, 0, 0).
\end{aligned}$$

Stability of the system against perturbations with wavelengths much longer than the width of the transition zone between the layers will be analyzed in the ideal MHD model. The linearized system of equations for small-amplitude oscillations developing near the equilibrium state in each domain is as follows:

$$\begin{aligned}
&\rho_{0j}\left(\frac{\partial \mathbf{v}_j}{\partial t} + (\mathbf{U}_{0j}\cdot\nabla)\mathbf{v}_j\right)\\
&= -\nabla\left(c_{sj}^2\tilde{\rho}_j + \frac{(\mathbf{B}_{0j}\cdot\mathbf{b}_j)}{4\pi}\right) + \frac{(\mathbf{B}_{0j}\cdot\nabla)\mathbf{b}_j}{4\pi},
\end{aligned} \tag{1}$$

$$\frac{\partial \mathbf{b}_j}{\partial t} + (\mathbf{U}_{0j}\cdot\nabla)\mathbf{b}_j = (\mathbf{B}_{0j}\cdot\nabla)\mathbf{v}_j - \mathbf{B}_{0j}(\nabla\cdot\mathbf{v}_j), \tag{2}$$

$$\frac{\partial \tilde{\rho}_j}{\partial t} = -\rho_{0j}\nabla\cdot\mathbf{v} - (\mathbf{U}_{0j}\cdot\nabla\tilde{\rho}_j). \tag{3}$$

Here, ρ_{0j} is the unperturbed plasma mass density in domain j; $c_{sj} = (\gamma T_e/M)^{1/2}$ is the ion acoustic velocity (with T_e, M, and γ being the electron temperature, ion mass, and adiabatic exponent, respectively); and $\mathbf{b}_j$, $\mathbf{v}_j$, and $\tilde{\rho}_j$ are small deviations of the magnetic field, velocity, and density from their equilibrium values $\mathbf{B}_{0j}$, $\mathbf{U}_{0j}$, and ρ_{0j}, respectively, in each of the domains $j = 1$, f, and 2. The solution to set of equations (1)–(3) is sought for in the form of plane waves,

$$F_j(z)\exp\left[i\left(-\tilde{\omega}t + k_x x + k_y y\right)\right], \tag{4}$$

where the components of the wave vector k_x and k_y are the same in all three domains. The complex amplitude $F_j(z)$ is represented as

$$\begin{aligned} F_1(z) &= C_1\exp\left[-k_1(z-a)\right], \\ F_2(z) &= C_2\exp\left[k_2(z+a)\right], \\ F_f(z) &= C_3\exp\left(k_f z\right) + C_4\exp\left(-k_f z\right), \end{aligned} \tag{5}$$

where C_1, C_2, C_3, and C_4 are constants. From Eqs. (1)–(3), we find the wavenumbers k_j ($j = 1, f, 2$) for each domain,

$$\begin{aligned} k_f^2 &= k^2\left(1 - \frac{(\cos\theta - \omega)^4}{(\cos\theta - \omega)^2\left(c_{sf}^2 + V_{Af}^2\right)/U_{0f}^2 - V_{Af}^2 c_{sf}^2\cos^2(\theta - \zeta_f)/U_{0f}^4}\right), \\ k_{1,2}^2 &= k^2\left(1 - \frac{\left(u_{1,2}\cos(\theta - \varphi_{1,2}) - \omega\right)^4}{\left(u_{1,2}\cos(\theta - \varphi_{1,2}) - \omega\right)^2\left(c_{s1,2}^2 + V_{A1,2}^2\right)/U_{0f}^2 - V_{A1,2}^2 c_{s1,2}^2\cos^2(\theta - \zeta_{1,2})/U_{0f}^4}\right). \end{aligned} \tag{6}$$

Here, $\omega = \tilde{\omega}/kU_{0f}$ (where $k \equiv \sqrt{k_x^2 + k_y^2}$ and U_{0f} is the flow velocity in the bounded layer $a > z > -a$) is the dimensionless frequency, θ is the angle between the wave vector and the x axis, and V_{Aj} is the Alfvén velocity in domain j.

In deriving the dispersion relation describing stability of the three-layer system under study, it is assumed that both the total (gas-kinetic plus magnetic) pressure and the plasma shift in the z direction are continuous at the interfaces $z = a$ and $z = -a$. The dispersion relation for solutions vanishing at $z \to \pm\infty$ has the form

$$(k_f^2 R_1 R_2 + k_1 k_2 R_f^2)\tanh(2k_f a) + k_f R_f(k_2 R_1 + k_1 R_2) = 0, \tag{7}$$

where $k_{1,2,f}$ are defined by Eqs. (6) and the following dimensionless functions are introduced:

$$\begin{aligned} R_1 &= \rho_1\left(u_1\cos(\theta - \varphi_1) - \omega\right)^2 - A_1\cos^2(\theta - \zeta_1), \\ R_2 &= \rho_2\left(u_2\cos(\theta - \varphi_2) - \omega\right)^2 - A_2\cos^2(\theta - \zeta_2), \\ R_f &= \left(\cos\theta - \omega\right)^2 - A_f\cos^2\left(\theta - \zeta_f\right), \\ A_f &= \frac{V_{Af}^2}{U_{0f}^2}, \quad A_1 = \frac{V_{A1}^2}{U_{0f}^2}\frac{\rho_{01}}{\rho_{0f}}, \quad A_2 = \frac{V_{A2}^2}{U_{0f}^2}\frac{\rho_{02}}{\rho_{0f}}, \\ u_1 &= \frac{U_{01}}{U_{0f}}, \quad u_2 = \frac{U_{02}}{U_{0f}}, \\ \rho_1 &= \frac{\rho_{01}}{\rho_{0f}}, \quad \rho_2 = \frac{\rho_{02}}{\rho_{0f}}. \end{aligned} \tag{8}$$

In the limit $k_f a \to 0$, Eq. (7) transforms into the dispersion relation for a system consisting of two plasmas separated by a plane interface [9]. For the case $\theta = \varphi_j = \zeta_j \equiv 0$, Eq. (7) coincides with the dispersion relation derived in [11]. Equation (7) is the general dispersion relation for the case of arbitrarily oriented magnetic fields and flow velocities in all domains. In this paper, we restrict ourselves to considering stability of a plasma flow propagating with a velocity U_{0f} in the bounded domain $-a < z < a$, assuming that the ambient plasma at $z > a$ and $z < -a$ is at rest. The magnetic fields in all three domains are directed along the x axis. Such a model adequately describes specific features of fast plasma flows propagating in the plasma sheet boundary layer of the Earth's magnetotail.

3. STABILITY OF A COMPRESSIBLE PLASMA FLOW PROPAGATING IN THE BOUNDED DOMAIN $a > z > -a$

3.1. Ambient Plasma Is Symmetric with Respect to the Flow

When the plasma parameters are the same on both sides of the flow ($R_1 = R_2$ and $k_1 = k_2$), general dispersion relation (7) is factorized,

$$\left(k_f R_1 + k_1 R_f\tanh\left(k_f a\right)\right)\left(k_1 R_f + k_f R_1\tanh\left(k_f a\right)\right) = 0. \tag{9}$$

Dispersion relation (9) has two types of solutions: symmetric (sausage-like) solutions, for which $k_1 R_f + k_f R_1\tanh\left(k_f a\right) = 0$, and antisymmetric (kink-like) ones, for which $k_f R_1 + k_1 R_f\tanh\left(k_f a\right) = 0$. It is well known that, at the interface between two semi-infinite plasmas propagating with respect to one another, wave perturbations vanishing at $z \to \pm\infty$ and propagating at small angles to the flow velocity can grow only if the ion acoustic velocity is sufficiently

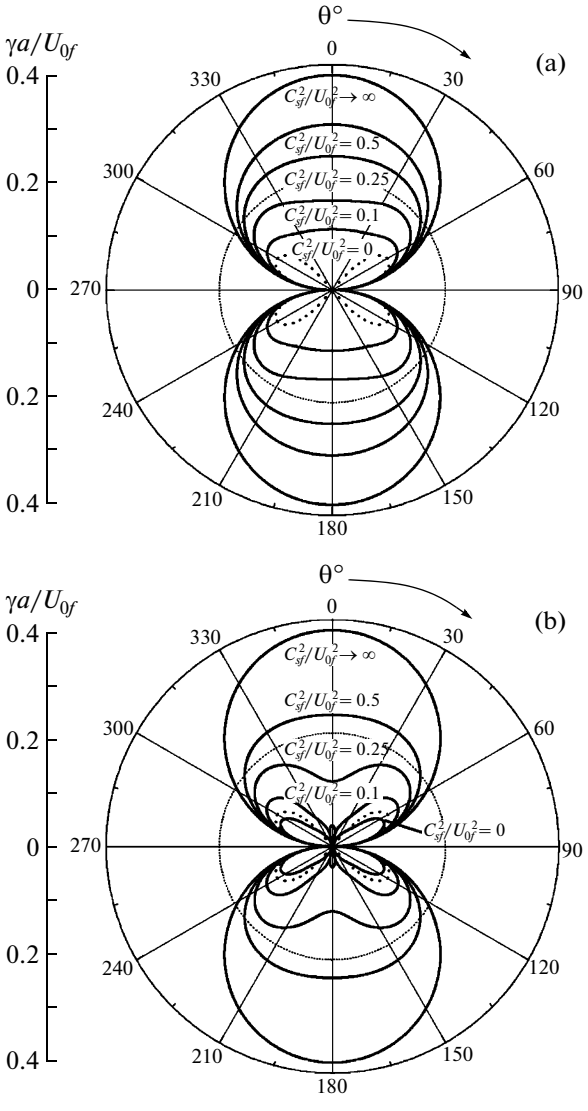

Fig. 2. Growth rates of (a) antisymmetric and (b) symmetric solutions to Eq. (9), normalized to U_{0f}/a, as functions of the angle θ for $ka = 1.0$ and different ion acoustic velocities. The plasma parameters are the same in all three domains, and $V_A/U_{0f} = 0.316$. The ratios of the squared ion acoustic velocity to the squared flow velocity are indicated in the figures. The dashed line shows the growth rate as a function of the angle θ for the case of two semi-infinite plasmas with $c_s = 0$.

high, $c_s > U_0/2 > V_A$ (see [9] and references therein). It follows from Eq. (9) that longitudinal perturbations ($\theta = 0$) with wavelengths much shorter than the flow width ($ka \gg 1$) can grow in a three-layer system only if $c_s > V_A$. However, as was shown in [11], longitudinal perturbations with wavelengths on the order of or longer than the flow width can grow in such a system due to the onset of KHI even for $c_s \to 0$.

Let us consider how the finite value of the ion acoustic velocity affects the dependence of the instability growth rate on the angle θ between the wave vector and the x axis. Figure 2 shows the results of numerical calculations of the perturbation growth rate for $ka = 1.0$ for the case in which the densities, temperatures, and magnetic fields are the same in all three domains, $\rho_1 = \rho_2 \equiv \rho = 1.0$, and $V_{Af}^2/U_{0f}^2 = V_{A1}^2/U_{0f}^2 = V_{A2}^2/U_{0f}^2 = 0.1$. The calculations were performed for different values of the ratio between the ion acoustic velocity and the flow velocity for both antisymmetric (Fig. 2a) and symmetric (Fig. 2b) solutions to dispersion relation (9).

It can be seen from Fig. 2 that the instability growth rate decreases with decreasing ion acoustic velocity, but remains positive even at $c_s \to 0$ for both the symmetric and antisymmetric modes. However, for $c_s < U_0/2$, the growth rate of the antisymmetric mode is substantially higher and this mode is unstable at any angle, including $\theta = 0$. For comparison, the dashed line in Fig. 2 shows the dependence of the growth rate on the angle θ for the case of semi-infinite plasmas separated by a plane interface ($V_A/U_{0f} = 0.316$, $c_s = 0$). It can be seen that, in this case, waves propagating along or at small angles to the flow velocity do not grow. The growth rate of the symmetric mode at $c_s \to 0$ is almost zero within a certain angular interval near $\theta = 0$ and smaller than that for the case of two semi-infinite plasmas for other angles. Note that, in the case of two semi-infinite plasmas, the symmetric and antisymmetric modes coincide. Figure 3 shows the growth rate of the antisymmetric mode, normalized to U_{0f}/a, as a function of the dimensionless wavenumber ka for different values of the angle θ between the wave vector and the x axis. The plasma parameters are the same as in Fig. 2, but the ratio of the squared ion acoustic velocity to the squared flow velocity is fixed, $c_s^2/U_{0f}^2 = 0.001$. The dashed lines show the dependences $\gamma a/U_0$ on ka for the case of two semi-infinite plasmas with the same parameters, $V_A^2/U_0^2 = 0.1$ and $c_s^2/U_{0f}^2 = 0.001$. It can be seen that, for two low-temperature semi-infinite plasmas, generation of waves propagating at angles smaller than $\theta_{cr} \approx 45.5°$ is impossible. In the three-layer system under study, waves propagating at any angle with respect to the flow velocity can be generated. In this case, in the range of angles forbidden for the case of two semi-infinite plasmas, waves in the limited interval of wavenumbers are generated even without allowance for the finite width of the transition zone d between the flow and the ambient plasma. The finiteness of the ka range in which waves are unstable is the most pronounced for the case $\theta = 0$. It should be noted that, unlike the case of two semi-infinite plasmas, in which the instability domain begins from $k = 0$, wave perturbations in a three-layer system become unstable only starting from a certain value $k_{min} \neq 0$. Obviously,

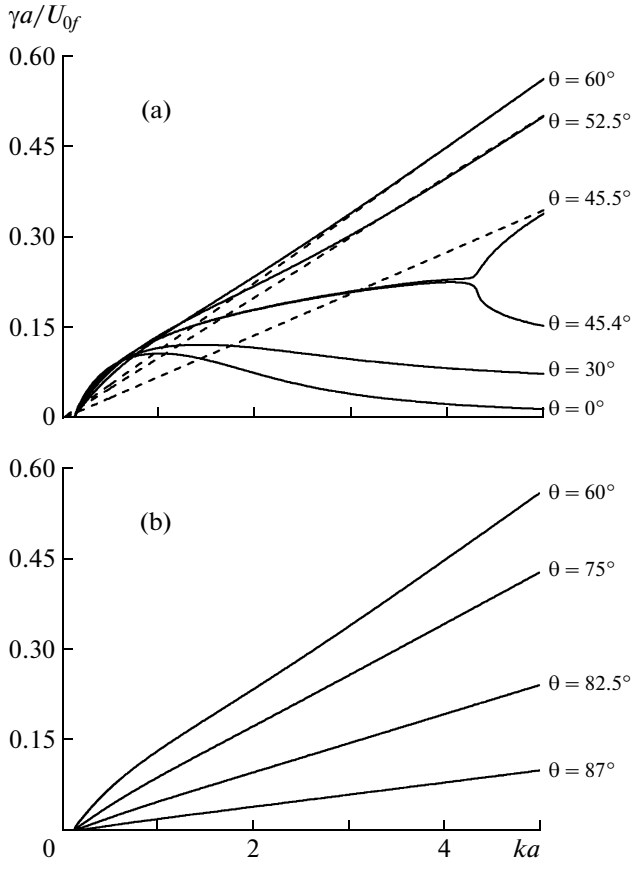

Fig. 3. Growth rate of the antisymmetric mode, normalized to U_{0f}/a, as a function of the dimensionless wavenumber ka for different angles θ. The plasma parameters are the same in all three domains: $V_A/U_{0f} = 0.316$, $c_s^2/U_{0f}^2 = 0.001$. The dashed lines in plot (a) show solutions for the case of two semi-infinite plasmas separated by a plane interface.

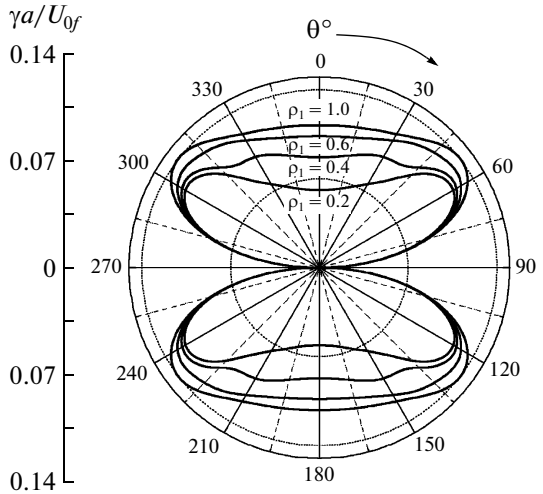

Fig. 4. Normalized growth rate as a function of the angle θ for $ka = 1.0$ and different ratios between the plasma densities in domain 1 and the flow, $\rho_1 = \rho_{01}/\rho_{0f}$. The plasma parameters and the magnetic field in domain 2 are the same as in the flow.

for $d \ll a$, the growth rates of waves propagating along or at small angles to the x axis, calculated with allowance for the width of the transition zone, will insignificantly differ from those calculated under the assumption $d = 0$.

For angles θ larger than θ_{cr}, the growth rate depends almost linearly on the wavenumber. In this case, the larger θ, the less the dependence $\gamma(ka)$ deviates from linear, coinciding for short-wavelength oscillations with the solution for the case of two semi-infinite plasmas. However, in the limit $ka \to 0$, the three-layer system remains stable for any propagation angle, unlike the case of two semi-infinite plasmas, for which the instability growth rate increases linearly with wavenumber starting from $ka = 0$. The linear increase in the growth rate in the short-wavelength range is a well-known problem: it is related with ignoring the width of the transition layer between the domains with different plasma velocities. In [9], it was shown for the case of two semi-infinite plasmas that, when the transition layer is taken into account, the range of wavenumbers in which waves are unstable is finite. In this case, waves with $kd \approx 0.5$ (where d is the width of the transition layer) grow at the highest rate. It should be remembered that here we assume that $a \gg d$ and consider generation of waves with sufficiently long wavelength ($kd \ll 1$).

3.2. Ambient Plasma Is Asymmetric with Respect to the Flow

When the plasma parameters and/or absolute values of the magnetic fields on both sides of the flow are different, one should solve general dispersion relation (7). Let us consider several typical cases.

3.2.1. Let us examine solutions to dispersion relation (7) in the case in which the plasma density, Alfvén velocity, and ion acoustic velocity in domain 2 are equal to those in the plasma flow ($V_{Af}^2/U_{0f}^2 = V_{A2}^2/U_{0f}^2 = 0.1$ and $c_{sf}^2/U_{0f}^2 = c_{s2}^2/U_{0f}^2 = 0.01$). We assume that, in domain 1, the plasma is colder ($c_{s1}^2/U_{0f}^2 = 0.001$) and the magnetic field is determined from the condition that the sum of the gas-kinetic and magnetic pressures in the flow is equal to that in domain 1,

$$\rho_1 \frac{V_{A1}^2}{U_{0f}^2} = \frac{V_{Af}^2}{U_{0f}^2} - \frac{6}{5}\left(\frac{c_{S1}^2\rho_1 - c_{Sf}^2}{U_{0f}^2}\right). \qquad (10)$$

Figure 4 shows the growth rate normalized to U_{0f}/a as a function of the angle θ for a wave perturbation

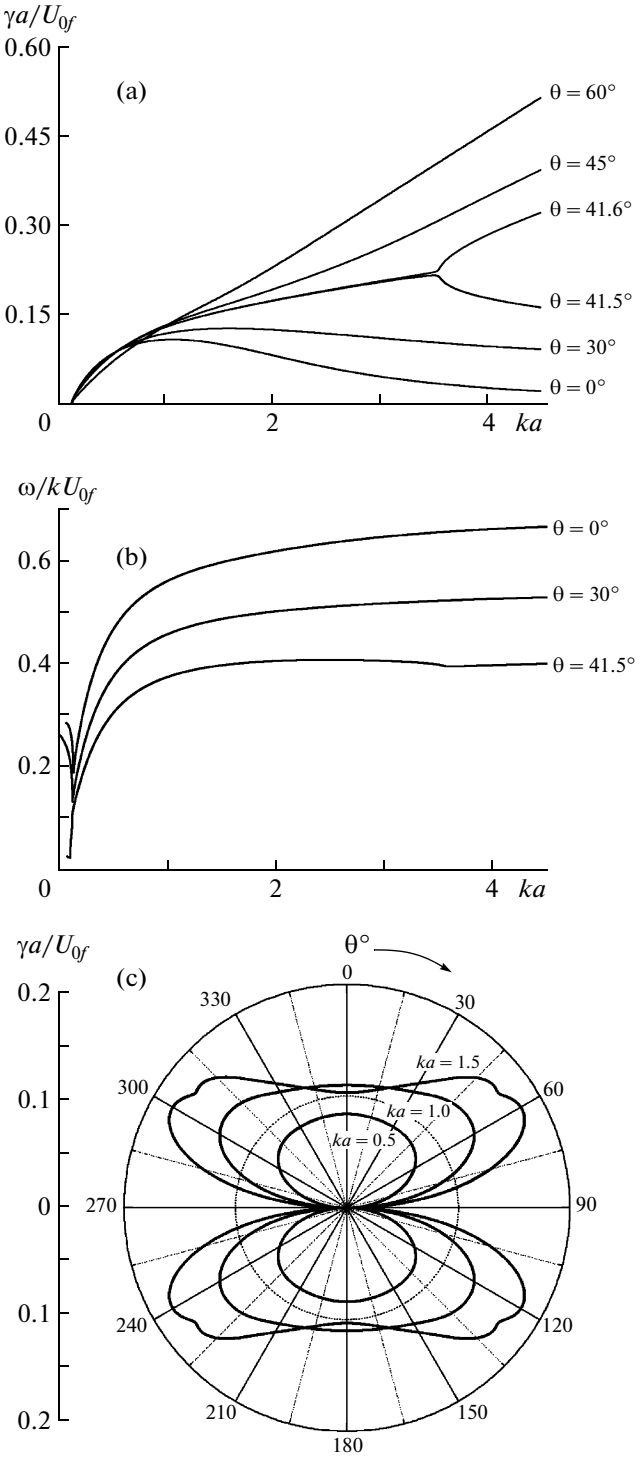

Fig. 5. Solutions to general dispersion relation (7) for the case of $V_{Af}/U_{0f} = 0.316$ and different plasma densities on both sides of the flow, $\rho_1 = 0.8$ and $\rho_2 = 1.2$. Plots (a) and (b) show the normalized growth rate $\gamma a/U_{0f}$ and normalized phase velocity ω/kU_{0f} as functions of ka for different values of θ, respectively, and plot (c) shows the normalized growth rate $\gamma a/U_{0f}$ as a function of the angle θ for three different values of ka.

with $ka = 1.0$. Only one solution to the dispersion relation is shown, because the second solution has a much smaller growth rate for waves propagating at angles $\theta < \theta_{cr}$. The calculations were performed for several values of the density ρ_1. We find from (10) that $V_{A1}/U_{0f} = 0.33$ for $\rho_1 = 1.0$, $V_{A1}/U_{0f} = 0.43$ for $\rho_1 = 0.6$, $V_{A1}/U_{0f} = 0.58$ for $\rho_1 = 0.4$, and $V_{A1}/U_{0f} = 0.75$ for $\rho_1 = 0.2$. The growth rate decreases with decreasing ρ_1 and, accordingly, increasing magnetic field in domain 1, because, for a stronger magnetic field, it is more difficult to bend the magnetic field lines. As the density increases, the growth rate increases to a certain maximum value and, then, decreases (see [11]). It should be noted that, for $\rho_1 = 0.2$, the flow velocity U_{0f} is lower than the sum of the Alfvén velocities in the flow and domain 1. In this case, a system consisting of two semi-infinite plasmas is stable against the onset of KHI. In the three-layer system, long-wave oscillations can be excited (see Fig. 4), because, at the interface between the flow and domain 2, the flow velocity U_{0f} is higher than the sum of the Alfvén velocities in the flow and domain 2; in this case, however, dispersion relation (7) has only one unstable solution.

3.2.2. Let us study solutions to general dispersion relation (7) for the case in which the plasma has different densities in all three domains. We use the parameters qualitatively reflecting the main characteristics of the plasma sheet boundary layer of the Earth's magnetotail, where a fast plasma flow propagates. For the flow, we assume $c_{sf}^2/U_{0f}^2 = 0.01$ and $V_{Af}/U_{0f} = 0.316$. For domain 1, simulating the cold rarefied lobe plasma, we take $\rho_{01}/\rho_{0f} = 0.8$ and $c_{s1}^2/U_{0f}^2 = 0.001$. The magnetic field is determined from the condition that the total (gas-kinetic plus magnetic) pressure in domain 1 is equal to that in the flow. Then, according to formula (10), we have $V_{A1}/U_{0f} = 0.373$. In domain 2, simulating the central plasma sheet, we take $\rho_{02}/\rho_{0f} = 1.2$ and $c_{s2}^2/U_{0f}^2 = 0.01$ and, accordingly, $V_{A2}/U_{0f} = 0.285$. The results of calculations are shown in Fig. 5. Figure 5a shows the growth rate normalized to U_{0f}/a as a function of ka for several values of θ. It can be seen that, similar to the case of equal parameters on both sides of the flow (Fig. 3), long-wavelength perturbations propagating at small angles with respect to the x axis grow in a limited range of wavenumbers and, accordingly, frequencies. We recall that it is in this angular range that wave generation due to the onset of KHI is impossible in a two-stream low-temperature plasma. It follows from Figs. 5a and 5c that the growth rates of wave perturbations propagating at sufficiently small angles with respect to the flow velocity ($\theta < 20^\circ$) is the highest at $ka \approx 1.0$. Oscillations with wavelengths longer than the flow width ($ka \le 0.5$) grow at

the highest rate if they propagate along the flow, as can be seen in Fig. 5c, which shows the normalized growth rate as a function of the angle θ for perturbations with different wavenumbers, $ka = 0.5$, 1.0, and 1.5. Waves propagating at sufficiently large angles with respect to the flow velocity ($\theta \geq 30°$) should be analyzed with allowance for the finite width of the transition layer (see the remark made in Section 3.2.1). However, when the width of the transition region is much smaller than the flow width, they should play a minor role in the generation of long-wavelength oscillations with $ka < 1.0$. Figure 5b shows the phase velocity normalized to the flow velocity U_{0f} as a function of ka. It can be seen that waves propagating along the flow have the maximum phase velocity.

3.2.3. Figure 6 shows the solutions to general dispersion relation (7) obtained for the same parameters as in Fig. 5, except for $V_{Af}/U_{0f} = 0.474$, i.e., for a magnetic field in the flow stronger (or a flow velocity lower) than that in the case considered in Section 3.2.2. According to Eq. (10), the ratios of the Alfvén velocities in the ambient plasma to the flow velocity also change. In domain 1, where $\rho_1 = 0.8$, we have $V_{A1}/U_{0f} = 0.543$ and, in domain 2, where $\rho_2 = 1.2$, we have $V_{A2}/U_{0f} = 0.431$. It should be noted that, in this case, the flow velocity is lower than the sum of the Alfvén velocities in the flow and domain 1, $U_{0f} < V_{Af} + V_{A1}$. It follows from the dispersion relation that, in this case (similar to the case presented in Fig. 4), the three-layer system can be unstable if the flow velocity is higher than the sum of the Alfvén velocities in the flow and domain 2. As was expected, an increase in the magnetic fields in the system and/or a decrease in the flow velocity leads to a substantial decrease in the instability growth rate. Moreover, for the parameters corresponding to Fig. 6, the system became more stable against the excitation of long-wave oscillations with $ka \leq 0.7$.

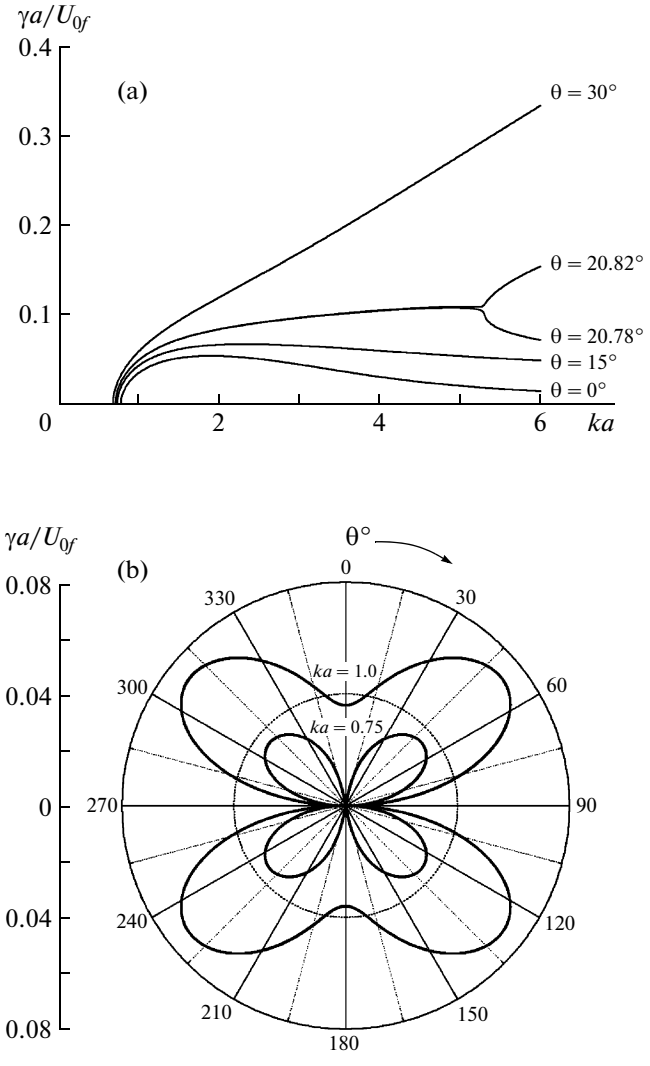

Fig. 6. Solutions to general dispersion relation (7) for the case of $V_{Af}/U_{0f} = 0.474$ and different plasma densities on both sides of the flow, $\rho_1 = 0.8$ and $\rho_2 = 1.2$. Plot (a) shows the normalized growth rate as a function of ka for different values of θ, and plot (b) shows the normalized growth rate as a function of the angle θ for $ka = 0.75$ and 1.0.

4. STRUCTURE OF EIGENMODES AND DEFORMATION OF THE FLOW BOUNDARIES

4.1. Components of the Magnetic and Electric Fields of the Wave

Let us denote a small deviation of the total (gas-kinetic plus magnetic) pressure from its equilibrium value as $\tilde{p} \equiv \left(c_{sj}^2\tilde{\rho}_j + \frac{(\mathbf{B}_{0j}\cdot\mathbf{b}_j)}{4\pi}\right)$, where $j = 1, 2, f$. Using Eqs. (1) and (2), we can express the components of the perturbed magnetic field $b_{x,y,z}$ and perturbed velocity $v_{x,y,z}$ in terms of $\tilde{p}$. When the plasma flow velocity is nonzero only in the bounded domain $-a < z < a$ and the magnetic fields in all domains are parallel to the flow velocity, we find that the components of the wave magnetic field are

$$b_{xj} = -\frac{B_{0j}\tilde{p}}{R_j\rho_{0f}U_{0f}^2}\left[\frac{k_j^2}{k^2} - \sin^2\theta\right],$$
$$b_{yj} = -\frac{B_{0j}\tilde{p}}{R_j\rho_{0f}U_{0f}^2}\cos\theta\sin\theta, \qquad (11)$$
$$b_{zj} = i\frac{B_{0j}\cos\theta}{kR_j\rho_{0f}U_{0f}^2}\frac{\partial\tilde{p}}{\partial z}$$

and the components of the perturbed velocity are

$$v_{xj} = \frac{\tilde{p}\cos\theta}{\rho_{0f}U_{0f}R_j}\left[\Omega_j + A_j\frac{k_j^2 - k^2}{k^2}\frac{1}{\rho_j\Omega_j}\right],$$
$$v_{yj} = -\frac{\Omega_j U_{0f}}{B_{0j}\cos\theta}b_{yj} = \frac{\tilde{p}\sin\theta}{\rho_{0f}U_{0f}R_j}\Omega_j, \qquad (12)$$
$$v_{zj} = -\frac{\Omega_j U_{0f}}{B_{0j}\cos\theta}b_{zj} = -i\frac{\Omega_j}{k\rho_{0f}U_{0f}R_j}\frac{\partial\tilde{p}}{\partial z},$$

where $\Omega_{1,2} = \omega$, $\Omega_f = (\omega - \cos\theta)$, and R_j and A_j are defined by formulas (8).

The components of the wave electric field can be obtained from the relationship $\mathbf{E} = -\frac{1}{c}\mathbf{V}\times\mathbf{B}$, where c is the speed of light. Obviously, if the magnetic fields and the flow velocity are directed along the x axis, then the component of the perturbed electric field e_x is identically zero in all three domains, independently of the plasma parameters and wave propagation direction. The remaining pair of the electric field components can easily be expressed in terms of the components of the wave magnetic field,

$$e_{yj} = -\frac{U_{0f}}{c}\frac{\omega}{\cos\theta}b_{zj},$$
$$e_{zj} = \frac{U_{0f}}{c}\frac{\omega}{\cos\theta}b_{yj}. \qquad (13)$$

These formulas show how the components of the magnetic field b_z and b_y of the excited wave are related to the components of the electric field e_y and e_z.

4.2. Structure of Eigenmodes Propagating along the Flow, $\theta = 0$

Let us consider the structure of eigenmodes propagating along the flow velocity. It follows from Eqs. (11) and (13) that, in this case, the magnetic field component b_y and the corresponding electric field component e_z are absent in the wave field.

Figures 7 and 8 show the results of calculations for the case in which the plasma has the same parameters on both sides of the flow and $V_A/U_{0f} = 0.316$ (see Section 3.1, Fig. 2). In this case, there are two eigenmodes, antisymmetric and symmetric. The distributions of the pressure and the transverse components of the magnetic and electric fields in these modes are shown in Figs. 7 and 8, respectively, for two typical values of the ratio between the ion acoustic velocity and the flow velocity. The heavy and light curves show the structure of modes for $c_s \to \infty$ and $c_s^2/U_{0f}^2 = 0.1$, respectively. The calculations were performed for a wave perturbation with $ka = 1.0$ for the instant at which the absolute value of the total perturbed pressure at the flow boundaries in the given cross section of the flow is at maximum. Figure 7a shows the profile of the total perturbed pressure normalized to its maximum value, $\delta p = \tilde{p}/\tilde{p}_{\max}$, along the z coordinate normalized to the half-width a of the flow for the antisymmetric mode, and Figs. 7b and 7c show the profiles of the real parts of the normalized components of the magnetic $(\delta b_{x,z} = \frac{\rho_0 U_{0f}^2}{\tilde{p}_{\max}}\frac{b_{x,z}}{B_{0f}})$ and electric $(\delta e_y = \frac{\rho_0 c U_{0f}}{\tilde{p}_{\max}}\frac{e_y}{B_{0f}})$ fields, respectively, calculated by formulas (11) and (13). Similar profiles for the symmetric mode are shown in Fig. 8.

It can be seen from Figs. 7 and 8 that, at a high plasma temperature ($c_s \to \infty$), the perturbed pressure, perturbed magnetic field, and wave electric field decrease monotonically on both sides of the flow. In a low-temperature plasma ($c_s^2/U_{0f}^2 = 0.1$), the distributions have an oscillatory–damped transverse structure. In the antisymmetric mode, one or two oscillations with amplitudes much smaller than those inside the flow are observed in the ambient plasma. For the symmetric mode, the distributions execute a large number of oscillations that damp slowly and, accordingly, penetrate more deep into the ambient plasma. However, as was shown in Section 3.1, the oscillation growth rate of the antisymmetric mode in a low-temperature plasma is much higher than that of the symmetric one; hence, the maximum value of the total perturbed pressure $\tilde{p}_{\max}$, in terms of which $\delta p, \delta b, \delta e$, are expressed, is also substantially larger for the antisymmetric mode.

As was expected, the pressure δp is continuous at the flow boundaries $z/a = \pm 1$, because it is this condition (together with the continuity of plasma displacement ξ at the interfaces) that was used in deriving the general dispersion relation. In Figs. 7 and 8, the component δb_z of the wave magnetic field and the corresponding electric field component δe_y are also continuous at the flow boundaries $z/a = \pm 1$. This is because, in the case at hand, the external magnetic fields in the flow and the ambient plasma are the same. If we express the z component of the velocity in terms of the displacement ξ, then, in the linear approximation, we have $v_{zj} = -i\Omega_j\xi_{zj}U_{0f}k$. Comparing this relationship with the last formula in Eqs. (12) and taking into account that the plasma displacement in the z direction is continuous, we find that $b_{zj}/B_{0j} = b_{zf}/B_{0f}$. Thus, the discontinuity of the external magnetic field causes the discontinuity of the z component of the perturbed magnetic field and the y component of the wave electric field. The behavior of the magnetic field component b_x, directed along the external magnetic field, depends substantially on the plasma temperature. In a hot incompressible plasma ($c_s \to \infty$), all the wave-

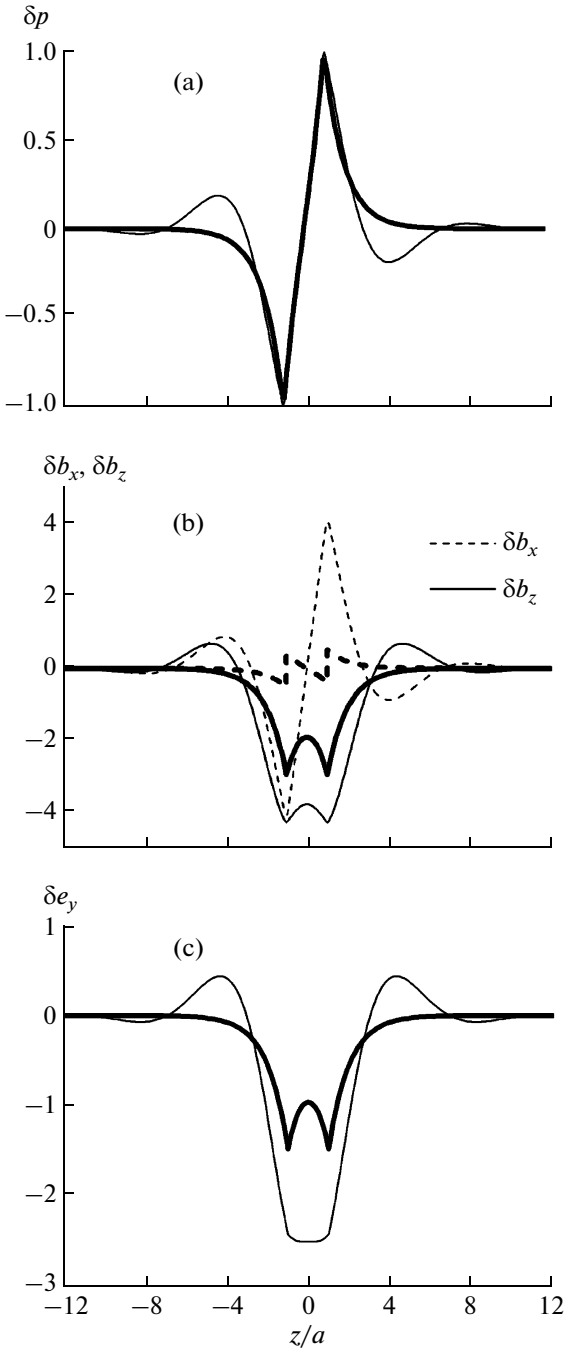

Fig. 7. (a) Pressure, (b) magnetic field components, and (c) electric field component as functions of z/a for an antisymmetric solution with $ka = 1$. The plasma parameters are the same in all domains, $V_A/U_{0f} = 0.316$. The heavy and light curves correspond to an incompressible plasma ($c_s \to \infty$) and a plasma with a finite ion acoustic velocity ($c_s^2/U_{0f}^2 = 0.1$), respectively.

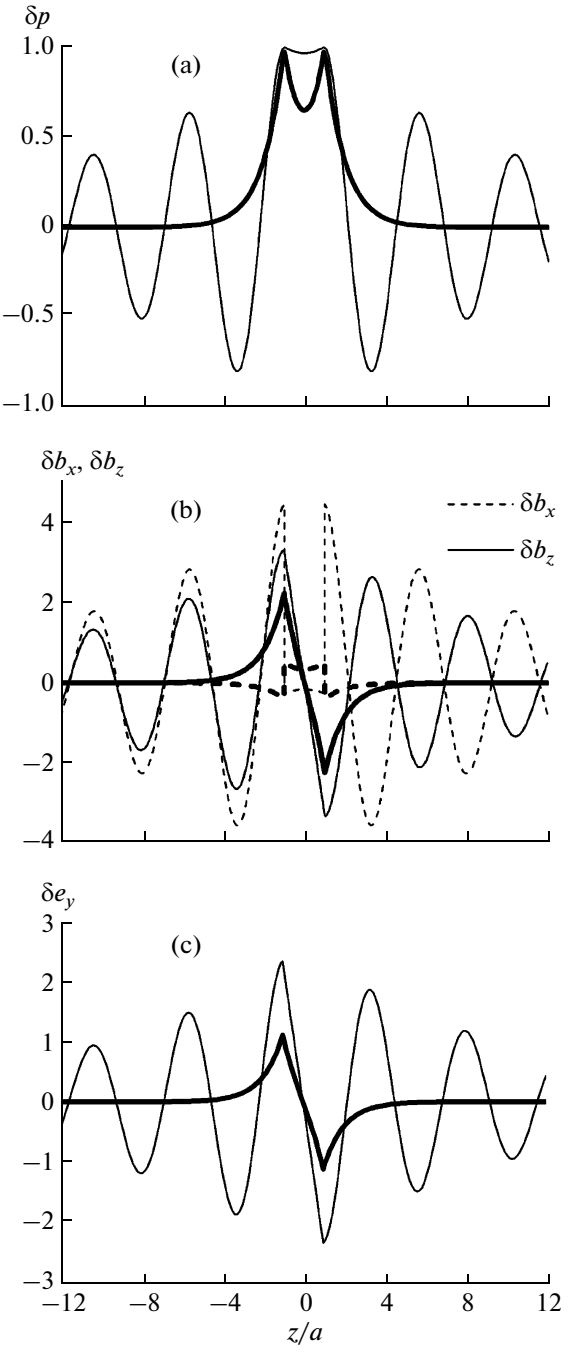

Fig. 8. (a) Pressure, (b) magnetic field components, and (c) electric field component as functions of z/a for a symmetric solution with $ka = 1$. The plasma parameters are the same in all domains, $V_A/U_{0f} = 0.316$. The heavy and light curves correspond to an incompressible plasma ($c_s \to \infty$) and a plasma with a finite ion acoustic velocity ($c_s^2/U_{0f}^2 = 0.1$), respectively.

numbers are the same, $k_f = k_1 = k_2 = \sqrt{k_x^2 + k_y^2} \equiv k$. In this case, we have $R_1 = R_2 \neq R_f$; then, it follows from Eqs. (11) that b_x has a discontinuity at the flow boundaries for both the symmetric and antisymmetric modes (see Figs. 7b, 8b). In a cold plasma ($c_s \to 0$), the behavior of b_x (see Eqs. (11)) is determined by the val-

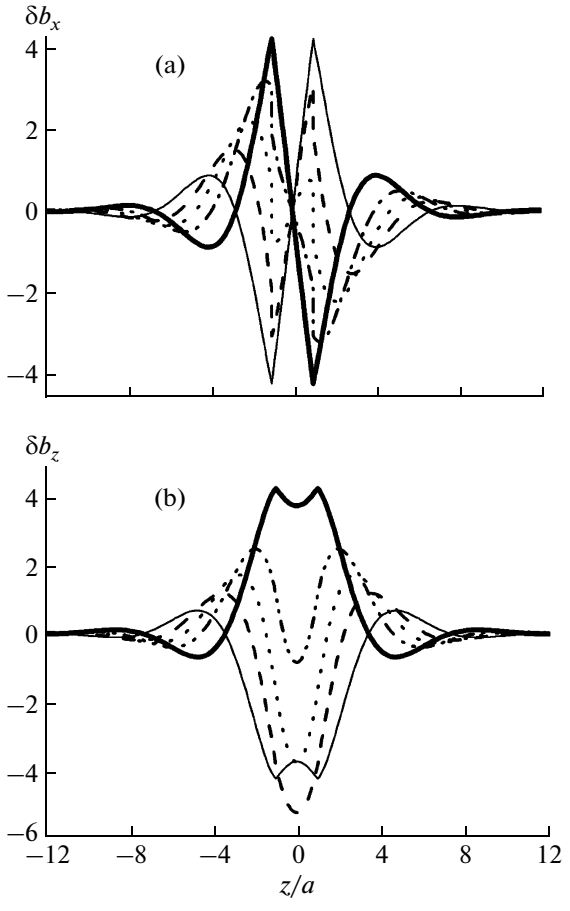

Fig. 9. Profiles of the magnetic field components (a) b_x and (b) b_z along the z axis in the antisymmetric mode propagating in a low-temperature plasma ($c_s^2/U_{0f}^2 = 0.1$) for different oscillation phases (see the text for details).

ues of the ratio k_j^2/R_j, $j = 1, f, 2$ at the flow boundaries $z/a = \pm 1$. It follows from formulas (6) and (8) that, for $\theta = 0$, the ratio k_j^2/R_j is continuous at the layer flow boundaries. Therefore, for waves propagating along the magnetic field, the component b_x is continuous. For perturbations propagating obliquely to the magnetic field, the real and imaginary parts of the component b_x (or one of them) are discontinuous at the flow boundaries, because, in this case, $k_1^2/R_1 = k_2^2/R_2 \neq k_f^2/R_f$. In the limiting case of an incompressible plasma, we have $b_x \ll b_z$ for both the symmetric and antisymmetric modes. As the temperature decreases, both b_x and b_z increase and become of the same order of magnitude in a low-temperature plasma ($c_s^2/U_{0f}^2 = 0.1$).

In Figs. 7 and 8, the results of calculations are presented for the instant at which the absolute value of the total perturbed pressure at the flow boundaries is at maximum. Since all the physical quantities related to the wave perturbation oscillate in time and space according to Eq. (4), their time behavior can be reconstructed by successively varying the oscillation phase. Figure 9 shows the z profiles of the magnetic field components for the antisymmetric mode in a low-temperature plasma ($c_s^2/U_{0f}^2 = 0.1$). Here, the light solid curves show the profiles of b_x and b_z presented in Fig. 7b; it is assumed that these curves corresponds to the phase $\Delta\varphi = 0$. The heavy dashed curves, light dashed curves, and dashed-and-dotted curves show the profiles of the magnetic field components for $\Delta\varphi = 0.3\pi$, 0.5π, and 0.7π, respectively. The heavy solid line shows the profiles constructed for the phase shift corresponding to one-half of the oscillation period, $\Delta\varphi = \pi$. Figure 9 clearly demonstrates the time behavior of the antisymmetric mode, which has an oscillatory–damped structure across the flow.

4.3. Structure of Eigenmodes Propagating Obliquely to the Flow Velocity

In a wave propagating obliquely to the flow velocity, all three magnetic field components, b_x, b_y, and b_z, and two electric field components, e_y and e_z, are nonzero. Figure 10 shows the profiles of the normalized magnetic field component $\delta b_y = \dfrac{\rho_0 U_{0f}^2}{\tilde{p}_{\max}} \dfrac{b_y}{B_{0f}}$ and the corresponding electric field component $\delta e_z = \dfrac{\rho_0 c U_{0f}}{\tilde{p}_{\max}} \dfrac{e_z}{B_{0f}}$, which are absent in a wave propagating along the flow. The calculations were performed for an antisymmetric mode propagating in a low-temperature plasma at an angle of $\theta = 10°$ to the flow velocity for the same parameters of the plasma system as in Fig. 7. The solid and dashed curves show the profiles of the real and imaginary parts of the field components, respectively, calculated by formulas (11) and (13). In this case, the discontinuities of the imaginary part of δb_y at the flow boundaries $z = \pm a$ cause the discontinuities of the real part of δe_z. The discontinuities of the imaginary part of δb_y follow from the fact that the quantity R_j ($j = 1, f, 2$) (see Eqs. (8)), through which the y component of the magnetic field is expressed in Eqs. (11), is discontinuous at the flow boundaries $z = \pm a$.

Let us consider the structure of the eigenmodes corresponding to the solutions to dispersion relation (7) obtained in Section 3.2.2 for the case in which the plasma densities and temperatures are different in all three domains: $\rho_{01}/\rho_{0f} = 0.8$, $c_{s1}^2/U_{0f}^2 = 0.001$, $\rho_{02}/\rho_{0f} = 1.2$, $c_{s2}^2/U_{0f}^2 = 0.01$, $V_{Af}/U_{0f} = 0.316$, and $c_{sf}^2/U_{0f}^2 = 0.01$. According to formula (10), the magnetic fields in domains 1 and 2 are different, $V_{A1}/U_{0f} = 0.373$ and $V_{A2}/U_{0f} = 0.285$. Figure 11 shows the trans-

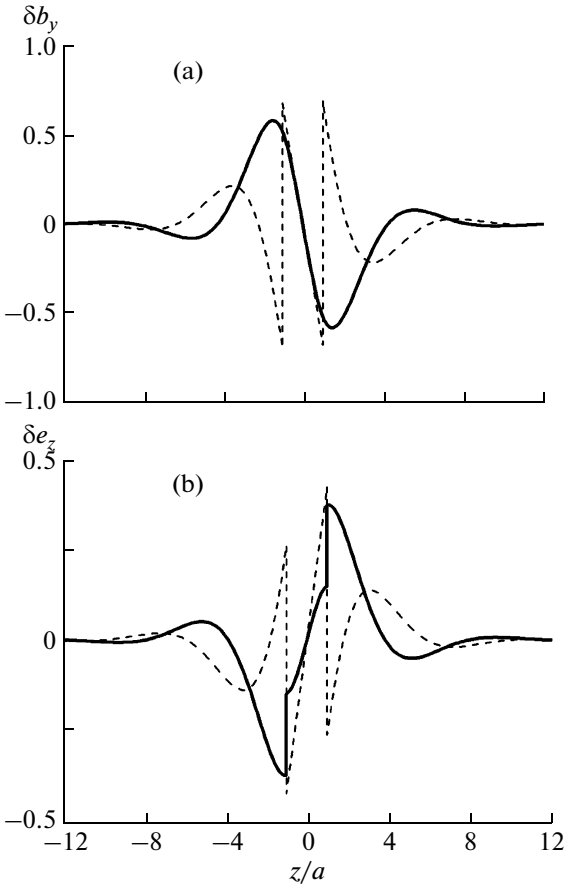

Fig. 10. Profiles of the (a) normalized magnetic field component δb_y and (b) normalized electric field component δe_z along the z axis in an antisymmetric mode with $ka = 1$, propagating at an angle of $\theta = 10°$ to the flow velocity. The solid and dashed curves show the real and imaginary parts of the field components, respectively. The plasma parameters are the same as in Fig. 7.

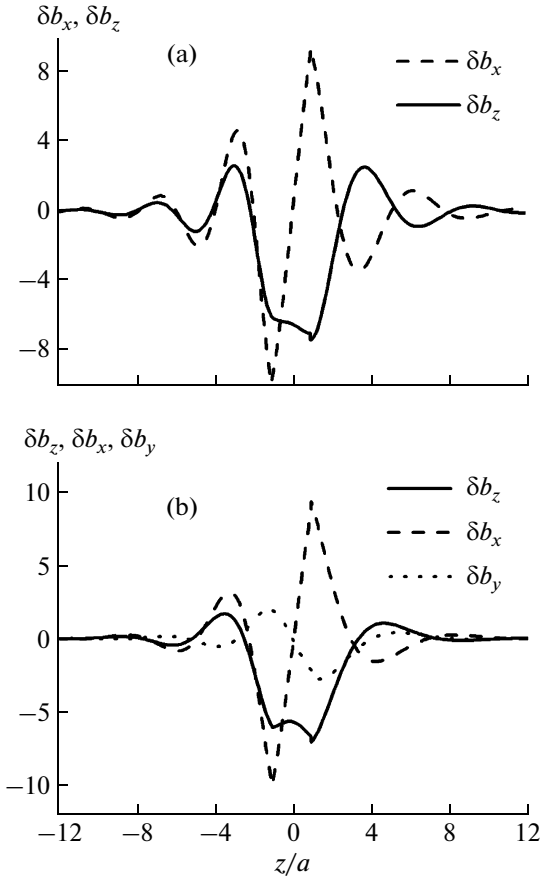

Fig. 11. Profiles of the normalized magnetic field components δb_x, δb_y, and δb_z corresponding to the solutions to dispersion relation (7) (see Fig. 5) for $ka = 1$ and $\theta =$ (a) 0° and (b) 30°.

verse profiles of the normalized magnetic field components in the asymmetric mode for waves propagating along the flow ($\theta = 0$, Fig. 11a) and at an angle of $\theta = 30°$ to the flow (Fig. 11b). In both cases, the transverse magnetic field component b_z is discontinuous at the flow boundaries $z/a = \pm 1$. As was discussed above, this discontinuity is caused by the discontinuity of the external magnetic field at the flow boundaries. As the wave propagation angle θ with respect to the flow increases, the b_z component of the magnetic field decreases monotonically, whereas the b_y component increases to its maximum value and, then, decreases according to formula (11).

4.4. Deformation of the Flow Boundaries

According to Eq. (4), the solutions considered in this study depend periodically on the coordinates x and y. If the plasma has the same parameters on both sides of the flow, the flow boundaries oscillate in the z direction either in phase (antisymmetric, or kink-like, eigenmodes) or in antiphase (symmetric, or sausage-like, eigenmodes). In the general case of arbitrary plasma parameters, the eigenmodes are asymmetric and the flow boundaries can oscillate with different amplitudes and phases. It was shown in [11] that, for the parameters typical of the plasma sheet boundary layer, oscillations propagating along the flow correspond to kink-like deformations of the flow. Figure 12 shows the displacements of the flow boundaries $\xi_{1,2}$ in the z direction, normalized to the maximum displacement of the boundary between the flow and domain 1. The ratio $\xi_{1,2}/\xi_{1\max}$ is shown as a function of the ratio x/a for a wave perturbation with $ka = 1$ propagating at an angle of $\theta = 30°$ to the flow. The displacements in Fig. 12 correspond to the solutions shown in Fig. 5. For convenience of comparison, the profiles of both boundaries are superimposed. The boundary between the flow and domain 1 is shown by the solid line, and that between the flow and domain 2, by the dashed

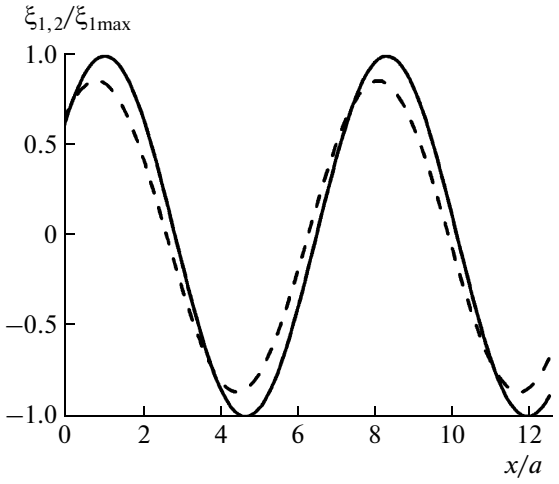

Fig. 12. Displacements of the flow boundaries $\xi_{1,2}$ along the z axis, normalized to the maximum displacement of the boundary between the flow and domain 1, as functions of x/a for a wave perturbation with $ka = 1$ propagating at an angle of $\theta = 30°$ to the flow velocity. The profiles of both boundaries are superimposed for convenience of comparison. The boundary between the flow and domain 1 is shown by the solid line, and that between the flow and domain 2, by the dashed line. The parameters of the plasma system are the same as in Figs. 5 and 11.

line. It can be seen that, similar to the case of wave perturbations propagating along the x axis ($\theta = 0$), the flow boundaries oscillate in close phases. In Fig. 12, the displacements of the flow boundaries are shown for the case in which the flow velocity is higher than the sum of the Alfvén velocities in the flow and domain 1 or 2 and the amplitude of oscillations of the upper boundary is larger than that of oscillations of the lower boundary. For boundary displacements corresponding to the case considered in Section 3.2.3 (the flow velocity is lower than the sum of the Alfvén velocities in the flow and domain 1, but higher than the sum of the Alfvén velocities in the flow and domain 2), the amplitude of oscillations of the upper boundary is smaller than the that of oscillations of the lower boundary, but the flow again undergoes kink-like deformation, i.e., the boundaries oscillate in close phases.

5. CONCLUSIONS

KHI in a plane three-layer geometry has been analyzed with allowance for plasma compressibility. A general dispersion relation for the case of arbitrarily oriented magnetic fields and flow velocities in the layers has been derived. Stability of a plasma flow propagating in the bounded domain has been considered in detail under the assumption that the ambient plasma is at rest and the magnetic fields in all three domains are directed along the flow velocity. Such a three-layer model adequately describes specific features of fast plasma flows propagating in the plasma sheet boundary layer of the Earth's magnetotail.

The experimental data obtained in the course of the *CLUSTER* multisatellite project were thoroughly analyzed in [5, 10]. It was shown in [10] that, the propagation of fast plasma flows along the magnetic field in the plasma sheet boundary layer is accompanied by magnetic field oscillations also propagating along the magnetic field. The flow velocities were found to be more than twice as high as the local Alfvén velocity, the oscillations had the shape of a kink-like mode, and the oscillation wavelengths were in the range of 5–20 Earth's radii.

Although the three-layer model is rather simplified, analysis of KHI in such a model makes it possible to explain almost all characteristic features of the phenomena observed. In our opinion, the most important result is that perturbations with wavelengths on the order of or larger than the flow width can grow in an arbitrary direction even at a zero temperature. This result differs drastically from the commonly considered case of two semi-infinite plasmas separated by a plane interface and propagating with respect to one another. In the latter case, there is a range of angles near the direction of the flow velocity in which wave generation in a low-temperature plasma ($c_s < V_A$) is impossible. In the three-layer plasma, long-wavelength oscillations can be excited at any angles. Calculations performed for the parameters close to the actual ones show that, in this case, oscillations with wavelengths longer than the flow width ($ka \le 0.5$) and propagating along the magnetic field grow at the highest rate. For a flow width of 3000 km, the wavelengths of these oscillations are longer than six Earth's radii, which agrees with the observed wavelengths (5–20 Earth's radii). Note that long-wavelength oscillations accompanying fast plasma flows propagate just along the magnetic field. Numerical calculations show that, in a low-temperature plasma, the growth rates of the eigenmodes resulting in kink-like deformations of the flow are much higher than those of eigenmodes resulting in sausage-like deformations. According to experimental data, oscillations in the plasma sheet boundary layer have the shape of a kink mode. Analysis of the structure of eigenmodes has shown that, at low plasma temperatures, the modes have an oscillatory-damped transverse structure. Unfortunately, the available experimental data are insufficient to determine the fine structure of long-wavelength oscillations excited by fast plasma flows propagating in the plasma sheet boundary layer.

ACKNOWLEDGMENTS

This work was supported by the Russian Foundation for Basic Research (project nos. 10-02-93115 and 10-02-00135), the Russian Federation State Contract no. 02.740.11.5064, and the Council of the Russian

Federation Presidential Grants for State Support of Leading Scientific Schools (grant no. NSh-3200.2010.2).

REFERENCES

1. H. Hasegawa, M. Fugimoto, T.-D. Phan, et al., Nature **430**, 755 (2004).
2. M. L. Nykyri, A. Otto, V. Lavraud, et al., Ann. Geophys. **24**, 2619 (2006).
3. M. Volwerk, R.-H. Glassmeier, R. Nakamura, et al., Geophys. Rev. Lett. **34**, L10 102 (2007).
4. K. Takagi, C. Hashimoto, H. Hasegawa, et al., J. Geophys. Res. **111**, A08 202 (2006).
5. E. E. Grigorenko, J.-A. Sauvaud, and L. M. Zeleny, J. Geophys. Res. **112**, A05 218 (2007).
6. A. M. Fridman, Usp. Fiz. Nauk **178**, 225 (2008) [Phys. Usp. **51**, 213 (2008)].
7. C. Uberoi, Planet. Space Sci. **34**, 1223 (1986).
8. K. W. Min, Astrophys. J. **482**, 733 (1997).
9. A. Miura and P. L. Pritchett, J. Geophys. Res. **87**, 7431 (1982).
10. E. E. Grigorenko, T. M. Burinskaya, M. Shevelev, et al., Ann. Geophys. **28**, 1273 (2010).
11. T. M. Burinskaya, Fiz. Plazmy **34**, 1013 (2008) [Plasma Phys. Rep. **34**, 936 (2008)].

Translated by E.G. Baldina